Network: Computation in Neural Systems
March–June 2014; 25(1–2): 3–19

informa
healthcare

On phasic inhibition during hippocampal theta

BRUCE P GRAHAM & EMILIANO SPERA

Computing Science & Mathematics, School of Natural Science, University of Stirling, Scotland, UK

(Received 30 September 2013; revised 7 January 2014; accepted 19 January 2014)

Abstract
Two computational models are used to explore the possible implications of recent experimental data (Royer *et al.* 2012) on phasic inhibition during theta frequency (4–10 Hz) oscillations in the hippocampi of actively behaving rodents. A working hypothesis from previous experimental and modelling studies is that a theta cycle is divided into encoding (when synaptic plasticity is enhanced) and recall (when plasticity is suppressed) half cycles. Using a compartmental model of a CA1 pyramidal cell, including dendritic spines, we demonstrate that out-of-phase perisomatic and dendritic inhibition, respectively, can promote the necessary conditions for these half cycles. Perisomatic inhibition allows dendritic calcium spikes that promote synaptic LTP, while minimising cell output. Dendritic inhibition, on the other hand, both controls cell output and suppresses dendritic calcium spikes, preventing LTP. The exact phase relationship between these sub-cycles may not be fixed. Using a simple sum-of-sinusoids activity model, we suggest an interpretation of the data of Royer *et al.* (2012) in which a fixed-phase encoding sub-cycle is surrounded by a flexible-phase recall cycle that follows the peak of excitatory drive and consequent phase precession of activity as an animal passes through a pyramidal cell's place field.

Keywords: *Oscillations, single neuron computation, synaptic plasticity*

Introduction

Theta oscillations (4–10 Hz) are prominent in rat (and other rodent) hippocampi during active behaviour and are likely to be functionally significant (Hasselmo 2005). Experimental and modelling studies suggest that a major role for theta is the separation in time of the processing of novel and familiar inputs

Correspondence: Bruce P Graham, Computing Science & Mathematics, School of Natural Science, University of Stirling, Scotland, UK. E-mail: b.graham@cs.stir.ac.uk

ISSN 0954-898X print/ISSN 1361-6536 online/04/010203–19 © 2014 Informa UK, Ltd.
DOI: 10.3109/0954898X.2014.886346

(Paulsen and Moser 1998; Hasselmo *et al*. 2002; Zilli and Hasselmo 2006; Manns *et al*. 2007; Cutsuridis *et al*. 2010; Cutsuridis and Hasselmo 2012). In this scenario, one half of a theta cycle is specialised for the encoding of new inputs through synaptic plasticity; whereas recall of previously stored associations is initiated on the alternate half cycle, and plasticity is restricted during this period. Experiments show that both spiking activity in hippocampal CA1 pyramidal cells (Manns *et al*. 2007) and the induction and reversal of synaptic long term potentiation (Hölscher *et al*. 1997; Hyman *et al*. 2003) are phasic with respect to theta and fit with this concept of differential processing of novel and familiar information.

It remains to be determined exactly how these functionally distinct theta half-cycles might arise, though they are likely the result of differential excitatory and inhibitory synaptic inputs between half-cycles (Hasselmo *et al*. 2002). In particular, different classes of inhibitory interneurons, driven by both external (feedforward) and internal (feedback) excitatory inputs in hippocampal area CA1 show strong phasic firing during theta (Klausberger *et al*. 2003; Klausberger *et al*. 2004; for overviews of this data see Cobb and Vida 2010; Klausberger and Somogyi 2008). The essential feature of this data is that inhibition is theta-phasic, with perisomatic inhibition, provided by basket (B) cells, strongest on the opposite phase of theta from dendritic inhibition, provided by bistratifed (BS) and oriens lacunosum-moleculare (OLM) cells. This corresponds to the idea that perisomatic inhibition could control cell output, while allowing synaptic plasticity to occur in the dendrites for the encoding of new information, whereas dendritic inhibition would filter the recall of familiar information and suppress synaptic plasticity (Paulsen and Moser 1998).

In this paper we use both simple and detailed computational models to provide further support for this hypothesis. In addition, recent experimental data on hippocampal ''place cell'' activity in awake, behaving animals, indicates that the theta-phasic relationships between excitatory and inhibitory inputs to a pyramidal cell may not be fixed, but can vary as a function of the animal's position relative to a cell's ''place field'' (Mizuseki *et al*. 2009; Royer *et al*. 2012). One consequence is that CA1 pyramidal cells show a phase precession of their firing, with spiking occurring earlier in a theta cycle as the animal passes through a cell's place field. One simple explanation for this is that it is due to changes in the relative strengths of CA3 and ECIII inputs that have distinct theta-phasic firing and separated, but overlapping place fields (Chance 2012), though a variety of cellular and network causes for phase precession have been proposed (see Chance 2012 for a discussion and references). A conceptually different scenario based upon the same principle is that ECIII input provides direct sensory signals, whereas the CA3 input forms a cue of remembered signals, so that EC input is strongest for novel stimuli, whereas CA3 input dominates for familiar stimuli, with the consequence that the preferred phase of CA1 activity shifts between the peak phases of EC and CA3 input depending on the familiarity of a sensory cue (Zilli and Hasselmo 2006; Manns *et al*. 2007). Here we explore how changes in phases of excitatory and inhibitory inputs affect the receiving cell's phasic activity during theta. The models, based on the place field data of Royer *et al*. (2012), suggest that the preferred theta phases of perisomatic and dendritic inhibition are labile, with the theta phase of new pattern encoding being somewhat fixed, but with the preferred phase of pattern recall shifting across the remainder of the theta cycle in response to behaviour.

Methods

Sum-of-sinusoids model

The essential characteristics of the effects of theta-modulated excitatory and inhibitory inputs on cell activity can be illustrated using a simple ''sum-of-sinusoids'' (SoS) model (Hasselmo *et al*. 2002; Zilli and Hasselmo 2006). We are specifically interested in the subtractive influence of inhibition on the phasic output of a pyramidal cell. The activity of a CA1 pyramidal cell (PC) is given as the sum of excitation from CA3 pyramidal cells and EC layer III cells, minus the inhibitory contributions from perisomatic-targetting (P) and dendrite-targetting (D) inhibitory interneurons:

$$A = CA3 + EC - P - D, \tag{1}$$

where each input is a sinusoid of particular frequency (w), phase (p), amplitude (a) and offset (o):

$$\text{Input}(t) = a \cdot \sin(wt - p) + o. \tag{2}$$

In the results shown, a unit frequency is assumed for all the inputs, corresponding to modulation at the same theta frequency. Phases and offsets are set to model particular combinations of inputs (see figure captions). Calculations of this model were carried out with Matlab (www.mathworks.com).

CA1 pyramidal cell compartmental model

To explore possible variations in synaptic plasticity due to inhibition during theta, we use a detailed compartmental model of a CA1 pyramidal cell (PC). The model is based on Migliore *et al* (2005), using cell morphology n5038804. The model contains fast sodium (Na), delayed rectifier potassium (K_{DR}), A-type potassium (K_A), anomalous rectifier ''h'', R-type calcium (Ca_R) and calcium-activated mAHP membrane ion channel currents. The soma contains Na and K_{DR}. Dendrites contain a uniform distribution of Na, K_{DR}, Ca_R and mAHP, and an increasing density of K_A and h up to 350 μm from the soma, beyond which the densities saturate. Excitatory synapses are formed on spines that are randomly distributed in the dendrites. Excitatory inputs stimulate AMPA and NMDA receptor-mediated responses, modelled as dual exponential current waveforms. Ten percent of the NMDAr current is assumed to be carried by calcium ions. Inhibitory synapses are placed on the soma and randomly distributed in the proximal apical dendrites. Inhibitory inputs stimulate $GABA_A$ receptor-mediated responses that are also modelled as dual exponential current waveforms. A full specification of the model is given in the appendix. This model was simulated using the NEURON software environment (www.neuron.yale.edu).

Results

Theta-modulated excitatory input

Cortical pyramidal cells receive distinct excitatory inputs from at least two sources. Hippocampal CA1 pyramidal cells (PCs) receive major excitation from CA3

pyramidal cells in the basal and proximal apical dendrites and from EC layer III cells in the distal apical tuft. The experimental data of Mizuseki *et al.* (2009) indicates that the preferred firing phase of CA1 PCs does not, on average, follow the peak firing phase of either the EC or CA3 inputs, but lies in between these peaks. However, a subset of fast firing CA1 PCs does closely follow the activity of similarly fast firing CA3 PCs (Mizuseki *et al.* 2009). Figure 1 clearly illustrates how the phase of peak PC activity may vary between the peaks of CA3 and EC activity, depending on the relative strengths of these inputs, using the simple SoS model. Here, the increased strength of an input pathway could correspond to greater population activity with the same mean cell firing rates, or it could represent more spikes due to faster firing of a subpopulation of cells.

The phase of peak output activity as a result of two sinusoidal inputs can be calculated directly from the formula (Zilli and Hasselmo 2006; Chance 2012):

$$\varphi = \tan^{-1} \frac{A_1 \sin \varphi_1 + A_2 \sin \varphi_2}{A_1 \cos \varphi_1 + A_2 \cos \varphi_2}, \tag{3}$$

where the two inputs have amplitudes A_1 and A_2 and phases φ_1 and φ_2, respectively. The phase precession of the output activity as the fractional contribution of a particular excitatory input is increased is illustrated in Figure 1c and is a sigmoidal function of the fraction. The recent model of phase precession in

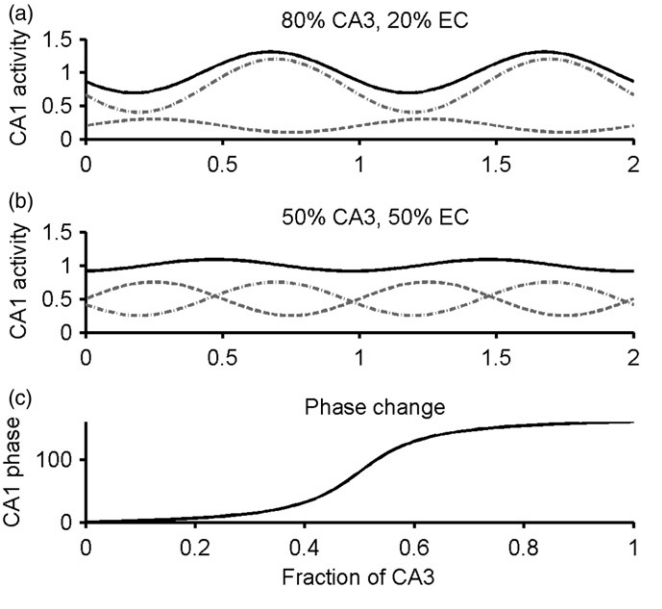

Figure 1. CA1 PC activity as a function of different proportions of theta-modulated, phased-offset, summed inputs from CA3 and EC. Inputs are sine waves of the form $I = k(0.5\sin(t\text{-}p) + 1)$ with EC phase $p = 0$ deg. and CA3 phase $p = 160$ deg. The scaling factor is set separately for CA3 and EC so that $k_{CA3} + k_{EC} = 1$. In plots (a) and (b), different proportions of EC (dashed line) and CA3 (dashed-dotted line) are summed to give CA1 activity (solid line): (a) $k_{CA3} = 0.8$, $k_{EC} = 0.2$; (b) $k_{CA3} = 0.5$, $k_{EC} = 0.5$. Two theta cycles are shown, running over a unit cycle time. (c) Mean phase of CA1 activity as a function of the fraction of CA3 activity (where EC + CA3 = 1 is the constant summed peak amplitude) calculated directly from Equation (3).

CA1 PC firing during theta by Chance (2012) is based on the PC receiving CA3 and EC excitation primarily at different phases of theta, and with different relative strengths, depending on an animal's position within a PC's ''place field''.

Inhibitory control of phasic firing

As discussed in Mizuseki *et al.* (2009), the preferred firing phase during theta is likely not simply a function of the relative strengths of phasic excitatory inputs, but will also be influenced by local circuit interactions as provided by the variety of feedforward and feedback inhibitory circuits identified in CA1 (Somogyi and Klausberger 2005). We use the SoS model to explore possible effects of inhibition on phasic CA1 PC activity.

Firstly, if the CA1 PCs receive a single dominant source of theta-modulated excitation then the CA1 activity will peak at the same theta phase as the input. Figure 2 demonstrates that theta-modulated inhibition can result in a phase shift in peak PC activity away from the peak of a single source of excitation. Without inhibition, or with inhibition 180 degrees out-of-phase with the excitation, peak PC

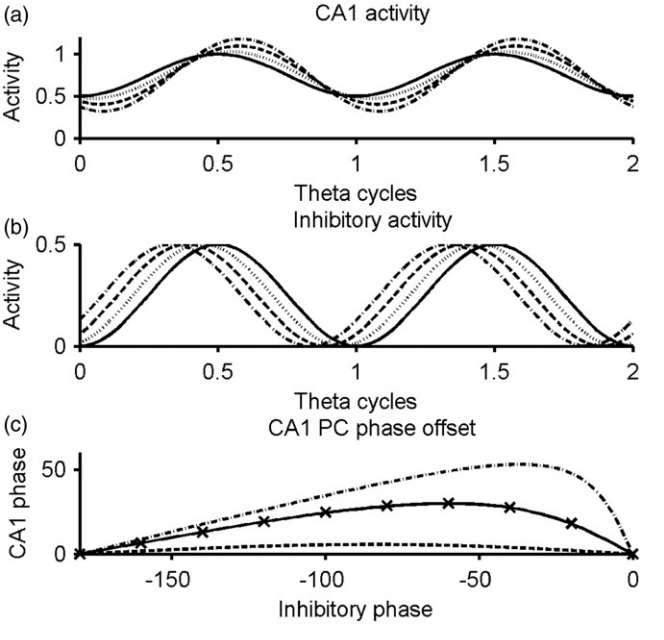

Figure 2. Effect of phase-offset inhibition on theta-modulated CA1 PC activity. PC activity is determined by a single sinusoidal excitatory input minus a sinusoidal inhibitory input. The excitatory input has amplitude a = 0.5, phase p = 90 degrees and offset o = 1.0. The inhibitory input has amplitude a = 0.25, offset o = 0.25, and phase varying between 0 (solid line), −20 (dotted), −40 (dashed), and −60 degrees (dot-dashed), relative to the excitatory phase. (a) PC activity corresponding to the different phases of inhibition shown in (b); (c) Phase lag, relative to the excitatory input, as a function of phase lead in the inhibition calculated using Equation (3): solid line is for inhibitory amplitude one half that of the excitatory amplitude (as in (a) and (b); crosses are phase offset taken from actual summed sinusoids); dashed line is inhibition set to 10% of excitation; dash-dotted line is inhibition set to 80% of excitation.

activity is in phase with the single source of excitation. However, a shift in the inhibitory phase away from the excitatory input phase results in a phase shift in peak PC activity in a direction opposite to peak of inhibition (Figure 2a,b). This shift reaches a maximum at a particular inhibitory phase advance, and then declines as the inhibitory phase is advanced to 180 degrees (Figure 2c). The maximum phase shift increases with the relative strength of the inhibition and occurs for an inhibitory peak closer to the excitatory peak for stronger inhibition. However, stronger inhibition also reduces the magnitude of theta modulation of the cell output, so though the phase shift is larger, the difference between maximum and minimum cell activity is reduced (effect can be seen in Figure 2a).

A CA1 PC receives inhibition through multiple pathways, with the basic categorisation being perisomatic (P) inhibition mediated by basket (B) cells and dendritic inhibition (D) from bistratified (BS) and oriens lacunosum-moleculare (OLM) cells (Somogyi and Klausberger 2005). The cell firing data of Klausberger, recorded from experiments in anaesthetized animals in which theta oscillations are induced by tactile stimulation (Klausberger *et al.* 2003; Klausberger *et al.* 2004), indicates that both P and D inhibition are strongly modulated at theta frequency, with the strengths of these forms of inhibition being largely out-of-phase with each other.

The simple SoS model would suggest that if P and D inhibition were of similar peak strength, in terms of inhibiting PC firing, but out-of-phase, then maximal inhibition would occur between the peaks of P and D firing. Figure 3 illustrates how such two out-of-phase sources of inhibition would produce phasic PC activity when the PC is driven by a constant (non-theta-modulated) source of excitation. Perfectly sinusoidal and 180 degrees out-of-phase inhibitory activity patterns would produce constant inhibition across a theta cycle (not shown). However, when the inhibitory inputs are not completely out-of-phase then peak PC activity lies in the trough between the inhibitory sources (Figure 3a). If one inhibitory source is significantly weaker than the other, then maximal PC activity is shifted towards the peak of the weaker inhibition (Figure 3b). The Klausberger data shows peak PC activity slightly lagging dendritic inhibition, which is in accord with dendritic inhibition having a weaker effect on PC spiking than perisomatic inhibition.

The recent experimental study of Royer *et al.* (2012) examined the differential effects during theta of perisomatic and dendritic inhibition in awake, behaving animals. They used optogenetic techniques to determine the effects of putative perisomatic and dendritic inhibition on CA1 PC place field activity in head-fixed mice running on a treadmill. A key result was that perisomatic inhibition caused a distinct phase shift in peak PC activity near the centre of a place field, but dendritic inhibition did not appear to affect PC phase (Royer *et al.*, Figure 7). Assuming the Chance (2012) model of PC phase precession, we use the SoS model to explore how the inhibition-mediated phase shifts seen by Royer *et al.* (2012) might arise. Here, the animal traversing the place field of a particular PC causes changes in the absolute and relative strengths of CA3 and EC excitatory inputs during the traversal. This is a result of the PC receiving inputs from CA3 and EC neurons that have overlapping, but spatially separated place field activity. The CA3 place fields are assumed to occur earlier along the linear track the animal traverses, so that CA1 PC activity is largely the result of CA3 inputs as the animal enters the PC's place field. In the centre of the place field, the PC receives strong input from both CA3 and EC,

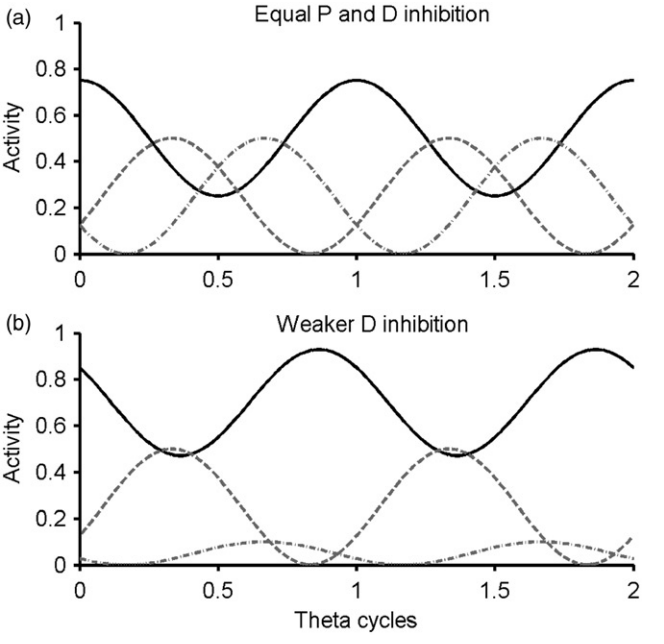

Figure 3. Effect of two inhibitory inputs on PC activity driven by constant excitation (amplitude 1 unit). (a) PC activity shown by solid black line. The two inhibitory inputs both have amplitude a = 0.25 and offset o = 0.25, but with a phase separation of 120 degrees (P: dashed line; D: dash-dotted line). (b) D inhibition amplitude reduced to 0.05 (with offset 0.05); lines as in (a).

Table I. Activity scaling factors for EC and CA3 inputs to mimic changes in the absolute and relative amplitudes of the two inputs as an animal traverses a place field. Bin number represents a spatial location in the linear place field.

Bin	1	2	3	4	5
EC	0.0620	0.3674	0.8947	0.8947	0.3674
CA3	0.3674	0.8947	0.8947	0.3674	0.0620

while on exit from the place field the input is largely from EC only. If both the CA3 and EC inputs are theta-modulated, but with the CA3 inputs having peak activity at a late theta phase compared to EC, then the CA1 PC shows a phase precession in peak activity from late to early theta phase as the animal moves through the place field (Chance 2012).

For comparison with the Royer *et al.* (2012) data, we consider place field activity at five different points (spatial bins) along the place field, corresponding to different absolute and relative amplitudes of peak CA3 and EC inputs (Table I). These points are postulated to model the causal inputs underlying the five spatial bins used to collate cell firing activity across a place field in the Royer paper. In addition to having separated, but overlapping place fields, the CA3 and EC inputs are theta-modulated but with different preferred phases, with CA3 peaking 160 degrees later in theta than the EC inputs (Figure 4a dashed and solid lines, respectively). The CA1 activity in the five spatial bins resulting from the summed excitation from CA3

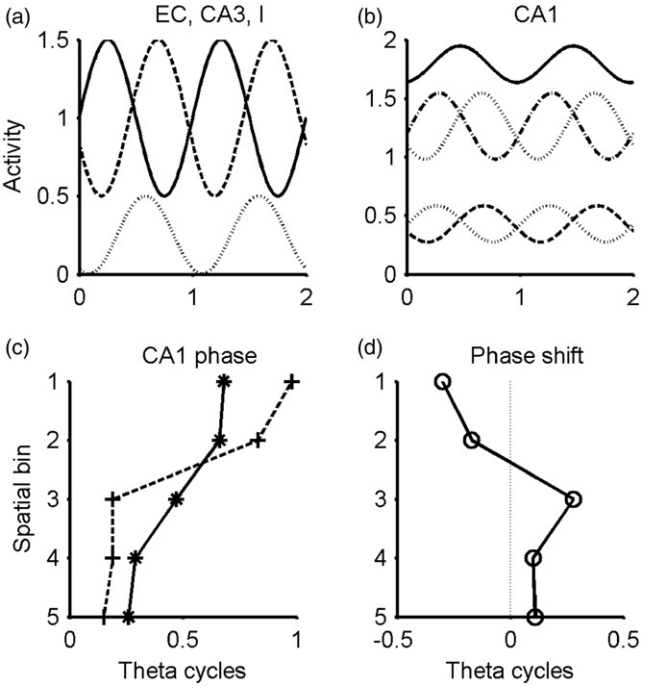

Figure 4. Effect of inhibition on CA1 PC activity determined by different amplitudes and proportions of two phase-offset excitatory inputs (EC and CA3). (a) Basic excitatory inputs have amplitude a = 0.5 and offset o = 1.0, with EC phase p = 0 degrees (solid line) and CA3 phase p = 160 degrees (dashed line). A single inhibitory input (I) with amplitude a = 0.25, offset o = 0.25 and phase p = 120 degrees (dotted line) when present is subtracted from the summed excitation to give the resultant PC activity. (b) CA1 PC activity for different amplitudes and proportions of CA3 and EC inputs, without inhibition (corresponding to different spatial bins in a place field; see Table I): dashed line is bin 1 (0.37 CA3 + 0.062 EC); upper dotted line is bin 2 (0.9 CA3 + 0.37 EC); solid line is bin 3 (0.9 CA3 + 0.9 EC); dot-dashed line is bin 4 (0.37 CA3 + 0.9 EC); lower dotted line is bin 5 (0.062 CA3 + 0.37 EC). (c) Theta phase of peak CA1 activity, plotted against spatial bin: solid line is with no inhibition; dashed line is with fixed phase inhibition (I shown as dotted line in (a)) subtracted from excitation. (d) Phase shift in peak CA1 activity due to inhibition (subtraction of dashed line from solid line in (c)). Phase and phase shift shown as fractions of a theta cycle in (c) and (d).

and EC, but with no inhibition, is shown in Figure 4b. The peak phase of CA1 activity in each bin is plotted in Figure 4c, which shows a rather linear phase precession to earlier theta phases through the centre of the place field (Figure 4b; cf Royer Figure 7a,c red lines and Chance Figure 2G). If there is a theta-modulated source of inhibition, with a phase slightly earlier than the peak phase of CA3 activity (Figure 4a dotted line), then this inhibition results in a distinct phase shift near the centre of the place field (when the excitatory contributions from EC and CA3 are similar) resulting in a much steeper transition from late (bin 2) to early (bin 3) theta firing (Figure 4c,d), which is comparable to that seen by Royer *et al.* (2012 Figure 7a,c blue lines). The phase shift when there is no inhibition compared to with inhibition, as a function of position (bin) across the place field is shown in Figure 4d, and is very similar in form to that shown in Royer Figure 7b, from experiments in which perisomatic inhibition is either blocked or present.

Royer *et al.* (2012) did not see a similar phase shift when dendritic inhibition was blocked. This suggests that dendritic inhibition does not have a fixed preferred theta phase (as that should cause a phase shift as illustrated here) but is either constant across theta, or remains in or out-of-phase with peak PC activity as this activity precesses in phase.

Theta-modulated synaptic plasticity

The above results only consider the effects of inhibition on cell firing (activity), with perisomatic and dendritic inhibition assumed to have similar effects. With the simple SoS model it is not possible to examine any differences in the effects of dendritic, as opposed to perisomatic inhibition that arise due to their particular spatial distribution within the target pyramidal cell. Though both forms of inhibition can attenuate EPSPs and thus control cell output spiking activity, they might play differential roles with respect to excitatory synaptic plasticity, since dendritic inhibition will keep a broader control of voltage transients across the dendrites than perisomatic inhibition. Further, in addition to phasic spiking activity across theta, experimental data also indicates that excitatory synaptic plasticity may be modulated across a theta cycle (Hölscher *et al.* 1997; Hasselmo *et al.* 2002; Hyman *et al.* 2003). To explore this phenomenon, and the possible contribution of different forms of inhibition to it, we use a detailed compartmental model of a CA1 PC. Excitatory synapses receiving spiking input generate a calcium transient in their postsynaptic spine due to calcium entry through NMDA receptors and through voltage-gated calcium channels (VGCCs). In the model, we take the amplitude of such calcium transients as a suitable indicator of the likelihood of long-term potentiation (LTP) occurring at a synapse.

In the compartmental model simulation, 100 excitatory (AMPA + NMDA) synapses on spines randomly distributed in the proximal apical dendrites (corresponding to CA3 input) each receive a synchronous ''theta-burst'' stimulus, consisting of 5 spikes at 100 Hz, similar to the stimuli used by Hölscher *et al.* (1997). Without inhibition, this combined input causes a prolonged calcium spike in the dendrites that propagates to the soma (Figure 5a) and results in a large calcium transient in each spine head (example trace shown in Figure 5e). Addition of gamma frequency (mean rate 100 Hz) stimulation to 10 inhibitory ($GABA_A$) synapses on the soma (P inhibition) and to 100 $GABA_A$ synapses randomly distributed in the proximal apical dendrites (D inhibition) spanning the arrival of the theta-burst excitation, inhibits the calcium spike and silences the cell (Figure 5b). The spine heads still experience a calcium transient due to calcium entry through NMDARs, but the amplitude and time course is much reduced (Figure 5f). If there is dendritic inhibition only, then the cell shows simple spiking output (Figure 5c) and a still small spine head calcium transient (Figure 5g). However, with somatic inhibition only, the cell fires a single simple spike (Figure 5d) but the spine head experiences a large calcium transient (Figure 5h) as calcium spiking in the dendrites is not inhibited.

In summary, perisomatic (P) inhibition can control cell firing activity while potentially allowing LTP at excitatory synapses in the dendrites due to large calcium transients in spine heads. Dendritic (D) inhibition, on the other hand, reduces both cell firing and synaptic plasticity by greatly reducing spine head calcium transients.

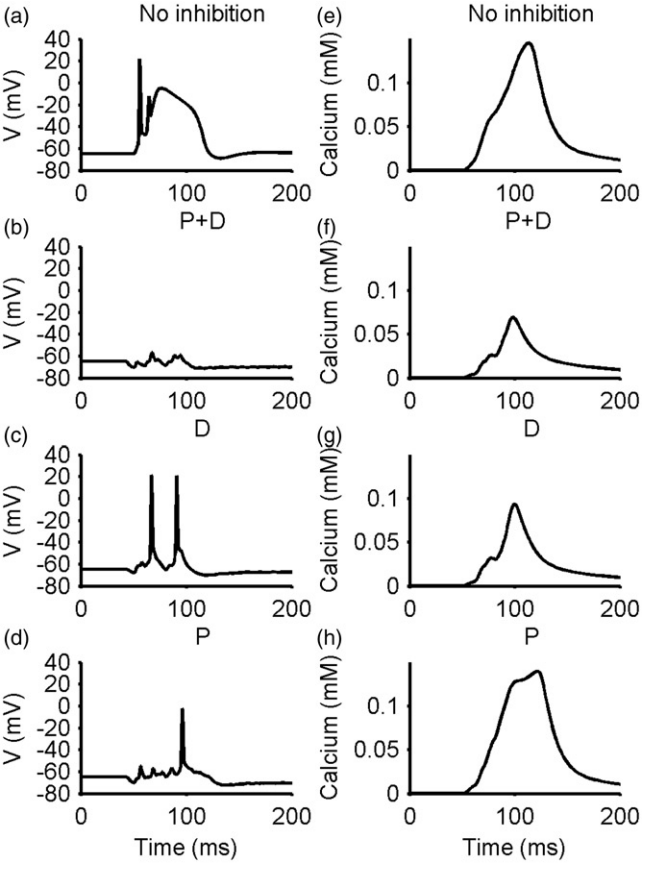

Figure 5. Somatic voltage and spine head calcium traces from a compartmental model of a CA1 PC during synchronous theta burst stimulation (5 spikes at 100 Hz) to 100 AMPA/NMDA synapses randomly distributed in the proximal apical dendrites. Bursts start at 50 msecs. Inhibition, when present, consists of noisy 100 Hz stimulation to 10 somatic (P) and 100 proximal apical dendritic (D) $GABA_A$ synapses, starting at 40 msecs and continuing throughout the excitatory burst stimulation. (a) somatic voltage trace with no inhibition; (b) somatic voltage with simultaneous P and D inhibition; (c) voltage with only D inhibition; (d) voltage with only P inhibition; (e–h) calcium traces in an example spine head receiving excitatory input, for different combinations of inhibition as per (a–d).

Thus if these two forms of inhibition are strongest at separate theta phases, the model predicts that LTP is most likely during the theta phase when perisomatic inhibition is strong, and less likely on the opposite phase when dendritic inhibition is strong. Spine head calcium transients during D inhibition may still be sufficient to induce LTD.

Discussion

Experimental data and computational modelling, including that presented here, demonstrate that a theta cycle is an ''information processing'' time window (of around 250 ms) during which novel and familiar inputs are ''processed'' in

different ways in distinct subwindows within the theta cycle (Hasselmo *et al.* 2002; Hasselmo 2005; Zilli and Hasselmo 2006). However, the exact mix and timing of cellular output and synaptic plasticity may vary between theta cycles for an individual pyramidal cell and across cell populations during active behaviour in an animal. This is the result of variation in the strength and theta-phases of at least two independent external excitatory input streams and multiple inhibitory pathways that are driven by these, and other, external inputs and by feedback excitation from the pyramidal cell population they inhibit. Recent complex models of networks of spiking neurons attempt to provide specific functional roles for these multiple excitatory and inhibitory pathways within a context of associative storage and recall (Cutsuridis and Hasselmo 2012; Cutsuridis *et al.* 2010). Here, using both simpler and more complex cellular models than employed in these network models, we have explored particular aspects of the differential contributions of perisomatic and dendritic inhibition to phasing cell output and synaptic plasticity during theta rhythms.

The simple sum-of-sinusoids model used here shows that phasic inhibition can significantly shift the peak of cellular activity away from the phase of the excitatory driving inputs (Figures 2, 3 and 4). Such a phase ''disconnect'' between input and output is seen in the data of Mizuseki *et al.* (2009) for hippocampal place cell activity. This relates directly to the ongoing question as to the coherence between theta rhythms in multiple connected areas, such as entorhinal cortex (EC), dentate gyrus (DG) and hippocampal areas CA3 and CA1. The Mizuseki data implies that low activity cells in CA1, firing only around a single spike per theta, may be most strongly controlled by local inhibition such that the preferred firing phase is largely independent of peaks in excitatory inputs from CA3 and EC. Higher firing cells in CA1 (around 40 Hz) are more tightly entrained to high firing inputs from CA3. Thus local inhibitory control can be overridden by sufficiently strong driving inputs (see, for example, Figure 3b).

A compartmental model of a CA1 pyramidal cell, in which calcium transients in dendritic spines were measured, confirms the intuition that increases in synaptic strength (LTP) are most likely to occur during periods of either complete disinhibition or at least when only perisomatic inhibition is strong. In these circumstances synaptic input can generate dendritic calcium spikes and large calcium transients in active spine heads, which would likely cause LTP. Dendritic inhibition suppresses these calcium spikes, and thus limits both LTP and cell firing, and may promote decreases in synaptic strength (LTD) through the smaller spine head calcium transients. The phasic separation in perisomatic and dendritic inhibition during theta (Klausberger *et al.* 2003; Klausberger *et al.* 2004) thus suggests that a theta cycle may be subdivided into encoding (storage) and retrieval subphases due to phasic inhibition. This concept has been used in network models of storage and recall in hippocampal area CA1, but with learning rules driven by regional voltage or calcium signals in the apical dendrites (Cutsuridis *et al.* 2010; Cutsuridis and Hasselmo 2012). We confirm here, with a detailed cellular model, that individual synapses will indeed experience different plasticity-driving signals between periods of perisomatic and dendritic inhibition.

However, our modelling based on the data of Royer *et al.* (2012) indicates that the phasic relationship between perisomatic and dendritic inhibition may not be constant. Taking the Chance (2012) model of phase precession as a basis, our

modelling suggests that the Royer *et al.* (2012) data may result from perisomatic (P) inhibition being theta-modulated with a fixed phase, whereas dendritic (D) inhibition follows the peak CA1 PC firing activity. The latter will arise if bistratified and OLM cells are largely driven by the same excitatory inputs as the PCs and by feedback excitation from the PCs, which is known to be the case (Klausberger and Somogyi 2008). This is consistent with recorded place preference and phase precession in inhibitory interneurons (Ego-Stengel and Wilson 2007). A constant phase of P inhibition provided by basket cells is more problematic, as it is driven by the same inputs as bistratified cells. This suggests that a further input modifies the preferred firing phase of BCs away from the peak of the excitatory drive to them, and the inhibitory inputs from the medial septum may do this (Klausberger and Somogyi 2008). Dendritic inhibition is always suppressed during high perisomatic inhibition, due to mutual inhibition between these inhibitory cell populations and possible preferential inhibition from different populations of medial septal cells (Cutsuridis and Hasselmo 2012). Thus recall and encoding will occur at different theta phases, but the phase separation will vary and can be less than 180 degrees.

To summarise this functional scenario, a portion of the theta cycle is dominated by P inhibition, with D inhibition being weak during this time. This results in strong control of PC output, while allowing for synaptic plasticity to take place in the dendrites. This window corresponds to a period when the PC is likely to be getting both CA3 and EC input, and these dual inputs are likely to determine plasticity within and between each pathway in a cooperative manner. Outside of this window, P inhibition is weak, allowing PC output firing, but this is accompanied by D inhibition, which is likely to restrict synaptic plasticity so that LTP is unlikely, but LTD may still occur. So even within a scenario of phase precession of CA1 PC firing as an animal moves through a PC's place field, the subdivision of theta cycles into sub-cycles of storage and recall may still hold, though now the phase of the peak recall shifts around the fixed phase of storage.

Much is still to be learnt about the functional consequences of the theta rhythm in the hippocampus. We do not directly address the interactions between storage of new and recall of old information here, but synaptic plasticity will change the role of a particular input pattern by either remembering it (LTP) or forgetting it (LTD) (Hasselmo *et al.* 2002). Such a change must alter the response of the target cell to subsequent presentations of that pattern, moving between novel and familiar responses, as determined by the theta-phase of the output (Zilli and Hasselmo 2006), or generating phase precession of the output during path traversal (Cutsuridis and Hasselmo 2012). Further work is still required to untangle the consequences of not just theta-phasic preferences for storage and recall, but of how this is affected by changes in phase preference of excitatory input pathways and intrinsic inhibitory pathways.

Declaration of interest: The authors report no conflicts of interest. The authors alone are responsible for the content and writing of the article.

References

Chance FS. 2012. Hippocampal phase precession from dual input components. The Journal of Neuroscience: The Official Journal of the Society for Neuroscience 32:16693–16703.

Cobb S, Vida I. 2010. Neuronal activity patterns in anaesthetized animals. In: Cutsuridis V, Graham B, Cobb S, Vida I, editors. Hippocampal microcircuits: A computational modeler's resource book. New York: Springer. pp 277–291.

Cutsuridis V, Hasselmo ME. 2012. GABAergic contributions to gating, timing, and phase precession of hippocampal neuronal activity during theta oscillations. Hippocampus 22:1597–1621.

Cutsuridis V, Cobb S, Graham BP. 2010. Encoding and retrieval in a model of the hippocampal CA1 microcircuit. Hippocampus 20:423–446.

Ego-Stengel V, Wilson MA. 2007. Spatial selectivity and theta phase precession in CA1 interneurons. Hippocampus 17:161–174.

Hasselmo ME. 2005. What is the function of hippocampal theta Rhythm? Linking behavioral data to phasic properties of field potential and unit recording data. Hippocampus 15:936–949.

Hasselmo ME, Bodelon C, Wyble BP. 2002. A proposed function for hippocampal theta rhythm: Separate phases of encoding and retrieval enhance reversal of prior learning. Neural Computation 14:793–817.

Hölscher C, Anwyl R, Rowan MJ. 1997. Stimulation on the positive phase of hippocampal theta rhythm induces long-term potentiation that can be depotentiated by stimulation on the ne. gative phase in area CA1 in vivo. The Journal of Neuroscience: The Official Journal of the Society for Neuroscience 17:6470–6477.

Hyman JM, Wyble BP, Goyal V, Rossi CA, Hasselmo ME. 2003. Stimulation in hippocampal region CA1 in behaving rats yields LTP when delivered to the peak of theta and LTD when delivered to the trough. The Journal of Neuroscience: the Official Journal of the Society for Neuroscience 23:11725–11731.

Klausberger T, Magill PJ, Marton LF, Roberts JDB, Cobden PM, Buzsaki G, Somogyi P. 2003. Brain-state- and cell-type-specific firing of hippocampal interneurons in vivo. Nature 421:844–848.

Klausberger T, Marton LF, Baude A, Roberts JDB, Magill PJ, Somogyi P. 2004. Spike timing of dendrite-targeting bistratified cells during hippocampal network oscillations in vivo. Nature Neuroscience 7:41–47.

Klausberger T, Somogyi P. 2008. Neuronal diversity and temporal dynamics: The unity of hippocampal circuit operations. Science 32:53–57.

Manns JR, Zilli EA, Ong KC, Hasselmo ME, Eichenbaum H. 2007. Hippocampal CA1 spiking during encoding and retrieval: Relation to theta phase. Neurobiology of Learning and Memory 87:9–20.

Migliore M, Ferrante M, Ascoli GA. 2005. Signal propagation in oblique dendrites in CA1 pyramidal cells. Journal of Neurophysiology 94:4145–4155.

Mizuseki K, Sirota A, Pastalkova E, Buzsáki G. 2009. Theta oscillations provide temporal windows for local circuit computation in the entorhinal-hippocampal loop. Neuron 64:267–280.

Paulsen O, Moser EI. 1998. A model of hippocampal memory encoding and retrieval: GABAergic control of synaptic plasticity. Trends in Neurosciences 21:273–278.

Royer S, Zemelman BV, Losonczy A, Kim J, Chance F, Magee JC, Buzsáki G. 2012. Control of timing, rate and bursts of hippocampal place cells by dendritic and somatic inhibition. Nature Neuroscience 15:769–775.

Somogyi P, Klausberger T. 2005. Defined types of cortical interneurone structure space and spike timing in the hippocampus. The Journal of Physiology 562.1:9–26.

Zilli EA, Hasselmo ME. 2006. An analysis of the mean theta phase of population activity in a model of hippocampal region CA1. Network: Computation in Neural Systems 17:277–297.

Appendix

Appendix: The compartmental model of the CA1 pyramidal cell is documented in the following tables.

A	Model Summary
Neuron model	Compartmental model of realistic CA1 pyramidal cell morphology with added spines
Channel models	Fast Na, K_{DR}, K_A, h, Ca_R, mAHP, Calcium concentration (Ca)
Synapse model	Conductance-based dual exponentials (AMPA) with voltage-dependence (NDMA); AMPA and NMDA co-localised at a synapse
Excitatory Input	100 Hz bursts of 5 spikes
Inhibitory Input	Mean 100 Hz with noisy interspike intervals
Measurements	Membrane potential and calcium concentration

B	Neuron model
Name	CA1 pyramidal cell
Type	Multicompartmental model
Morphology	Cell no. 5038804 from ModelDB accession no. 55035 (as described in Migliore et al., 2005); divided into 337 compartments as determined by frequency response criterion at 50Hz (Carnevale and Hines, 2006)
Spines	Spines with spine head 0.5 μm by 0.5 μm and spine neck 1.0 μm long by 0.125 μm wide added at random locations in the dendrites
Membrane potential	Standard compartmentalised cable equation
Passive properties	$R_m = 28\,000\,\Omega\,cm^2$; $R_a = 150\,\Omega\,cm$; $C_m = 1\,\mu F/cm^2$

C	Ion channels
Na	$I_{Na} = \bar{g}_{Na} m^3 hs(V - E_{Na})$ $\frac{dm}{dt} = \frac{(m_\infty - m)}{\tau_m}$; $\frac{dh}{dt} = \frac{(h_\infty - h)}{\tau_h}$; $\frac{ds}{dt} = \frac{(s_\infty - s)}{\tau_s}$ $a_m = 0.4(V+30)/(1 - e^{-(V+30)/7.2})$; $b_m = -0.124(V+30)/(1 - e^{(V+30)/7.2})$ $m_\infty = \frac{a_m}{a_m + b_m}$; $\tau_m = \max[\frac{1}{Q(a_m+b_m)}, 0.02]$ ms; $Q = Q10^{(T-24)/10}$ $a_h = 0.03(V+45)/(1 - e^{-(V+45)/1.5})$; $b_h = -0.01(V+45)/(1 - e^{(V+45)/1.5})$ $h_\infty = 1/(1 + e^{(V+50)/4})$; $\tau_h = \max[\frac{1}{Q(a_h+b_h)}, 0.5]$ ms $a_s = e^{\frac{96.48\varphi_s(V+60)}{8.315(273.16+T)}}$; $b_s = e^{\frac{96.48\varphi_s\gamma_s(V+60)}{8.315(273.16+T)}}$; $c_s = 1/(1 + e^{(V+58)/2})$ $s_\infty = c_s + \frac{a_r}{1-c_s}$; $\tau_s = \max[\frac{b_s}{0.0003(1+a_s)}, 10]$ ms $E_{Na} = 55$ mV; $\varphi_s = 12$; $\gamma_s = 0.2$; $Q10 = 1$; $T = 34\,^\circ$C $a_r = 1 - (0.5x)/350$ for distance $x < 350\,\mu m$ and $a_r = 0.5$ for $x > 350\,\mu m$ Present in all compartments (except spines): $\bar{g}_{Na} = 0.025$ S/cm^2 in soma and $\bar{g}_{Na} = 0.015$ S/cm^2 in dendrites
K_{DR}	$I_{KDR} = \bar{g}_{KDR} n(V - E_K)$ $\frac{dn}{dt} = \frac{(n_\infty - n)}{\tau_n}$ $a_n = e^{\frac{96.48\varphi_n(V - V_{hn})}{8.315(273.16+T)}}$; $b_n = e^{\frac{96.48\varphi_n\gamma_n(V - V_{hn})}{8.315(273.16+T)}}$ $n_\infty = \frac{1}{1+a_n}$; $\tau_n = \max[\frac{b_n}{0.02Q(1+a_n)}, 2]$ ms; $Q = Q10^{(T-24)/10}$ $E_K = -90$ mV; $V_{hn} = 13$ mV; $\varphi_n = -3$; $\gamma_n = 0.7$; $Q10 = 1$; $T = 34\,^\circ$C Present in all compartments (except spines): $\bar{g}_{KDR} = 0.01$ S/cm^2
K_A	$I_{KA} = \bar{g}_{KA} nl\,(V - E_K)$ $\frac{dn}{dt} = \frac{(n_\infty - n)}{\tau_n}$; $\frac{dl}{dt} = \frac{(l_\infty - l)}{\tau_l}$ $a_n = e^{\frac{96.48\varphi(V - V_{hn})}{8.315(273.16+T)}}$; $b_n = e^{\frac{96.48\varphi\gamma_n(V - V_{hn})}{8.315(273.16+T)}}$; $\varphi = \varphi_n - 1/(1 + e^{(V+40)/5})$ $n_\infty = \frac{1}{1+a_n}$; $\tau_n = \max[\frac{b_n}{Qa_0(1+a_n)}, 0.1]$ ms; $Q = Q10^{(T-24)/10}$ $a_l = e^{\frac{96.48\varphi_l(V - V_{hl})}{8.315(273.16+T)}}$; $l_\infty = \frac{1}{1+a_l}$; $\tau_l = \max[0.26(V+50), 2]$ ms; $E_K = -90$ mV; $Q10 = 5$; $T = 34\,^\circ$C

(*continued*)

Appendix. Continued.

Prox (<100 μm): $V_{hn} = 11\,\text{mV}$; $V_{hl} = -56$ mV; $\varphi_n = -1.5$; $\gamma_n = 0.55$; $a_0 = 0.05$; $\varphi_l = 3$

Distal (>100 μm): $V_{hn} = -1\,\text{mV}$; $V_{hl} = -56\,\text{mV}$; $\varphi_n = -1.8$; $\gamma_n = 0.39$; $a_0 = 0.1$; $\varphi_l = 3$

$\bar{g}_{KA} = g^*_{KA}(1+x)/100$ for distance $x < 350\,\mu m$ and $\bar{g}_{KA} = g^*_{KA}4.5/100$ for $x > 350\,\mu m$

Low K_A: $g^*_{KA} = 0.01\,\text{S/cm}^2$; High K_A: $g^*_{KA} = 0.03\,\text{S/cm}^2$

h

$I_h = \bar{g}_h l\,(V - E_h)$

$\frac{dl}{dt} = \frac{(l_\infty - l)}{\tau_l}$

$a_l = e^{0.0378\varphi_l\,(V - V_{hl})}$; $b_l = e^{0.0378\varphi_l\gamma_l\,(V - V_{hl})}$

$l_\infty = \frac{1}{1+e^{-(V-V_{hk})/k_l}}$; $\tau_n = \frac{b_l}{0.011Q(1+a_l)}$ ms; $Q = Q10^{(T-33)/10}$

$E_h = -30\,\text{mV}$; $V_{hl} = -73\,\text{mV}$ for distance $x < 100\,\mu m$ and $V_{hl} = -81\,\text{mV}$ otherwise; $\varphi_l = 2.2$; $\gamma_l = 0.4$; $V_{hk} = -81\,\text{mV}$; $k_l = -8$; $Q10 = 4.5$; $T = 34\,^\circ\text{C}$

Present in all compartments (except spines): $\bar{g}_h = g^*_h(1+3x)/100$ for distance $x < 350\,\mu m$ and $\bar{g}_h = g^*_h 11.5/100$ for $x > 350\,\mu m$; $g^*_h = 0.00005\,\text{S/cm}^2$

Ca_R

$I_{Ca} = \bar{g}_{Ca} m^3 h (V - E_{Ca})$

$\frac{dm}{dt} = \frac{(m_\infty - m)}{\tau_m}$; $\frac{dh}{dt} = \frac{(h_\infty - h)}{\tau_h}$

$m_\infty = \frac{1}{1+e^{(V-V_{hm})/k_m}}$; $\tau_m = 3.6\,\text{mS}$; $h_\infty = \frac{1}{1+e^{(V-V_{hh})/k_h}}$; $\tau_h = 20\,\text{mS}$

$E_{Ca} = 10\,\text{mV}$; $V_{hm} = -30\,\text{mV}$; $V_{hh} = -65\,\text{mV}$; $k_m = -6.7$; $k_h = 11.8$

In all compartments: $g_{Ca} = 0.03\,\text{S/cm}^2$

mAHP

$I_{mAHP} = \bar{g}_{mAHP} m (V - E_K)$

$\frac{dm}{dt} = \frac{(m_\infty - m)}{\tau_m}$

$\tau_m = \frac{1}{a_m + b_m}$; $m_\infty = a_m \tau_m$;

$E_K = -90\,\text{mV}$;

In all compartments: $g_{mAHP} = 0.001\,\text{S/cm}^2$

Ca	Calcium concentration as a function of calcium current, buffering and extrusion:
	$\frac{dCa}{dt} = \frac{\mathcal{J}_{Ca}}{1+b} + \frac{Ca_\infty - Ca}{\tau_{Ca}}$; $\mathcal{J}_{Ca} = \frac{-10000 I_{Ca}}{2Fd}$
	Instantaneous buffer capacity $b = 17$; extrusion time constant $\tau_{Ca} = 28.6\,\text{ms}$
	F is Faraday's constant (96 490 coulombs/mole); depth $d = 0.1\,\mu m$
	Steady state $Ca_\infty = 100\,\text{nM}$; Current I_{Ca} in mA/cm^2
D	Synapses
AMPA	$I_{AMPA} = g_{AMPA}(V - E_{AMPA})$
	$g_{AMPA} = \bar{g}_{AMPA} \frac{\tau_1 \tau_2}{\tau_2 - \tau_1} (e^{-t/\tau_2} - e^{-t/\tau_1})$
	$\tau_1 = 0.5\,\text{ms}$; $\tau_2 = 3\,\text{ms}$; $E_{AMPA} = 0\,\text{mV}$
	$\bar{g}_{AMPA} = 0.5\,\text{nS}$
NMDA	$I_{NMDA} = g_{NMDA}(V - E_{NMDA})$
	$g_{NMDA} = \bar{g}_{NMDA} f s (e^{-t/\tau_2} - e^{-t/\tau_1})$
	$f = 1/(e^{-\tau_p/\tau_2} - e^{-\tau_p/\tau_1})$; $\tau_p = \frac{\tau_1 \tau_2}{\tau_2 - \tau_1} \ln(\tau_2/\tau_1)$
	$s = 1/(1 + \mu[Mg^{2+}]e^{-\gamma V})$
	$\mu = 0.33$; $[Mg^{2+}] = 1\,\text{mM}$; $\gamma = 0.06/\text{mV}$
	$\tau_1 = 3\,\text{ms}$; $\tau_2 = 150\,\text{ms}$; $E_{NMDA} = 0\,\text{mV}$
	$\bar{g}_{NMDA} = 1\,\text{nS}$
GABA$_A$	$I_{GABA} = g_{GABA}(V - E_{GABA})$
	$g_{GABA} = \bar{g}_{GABA} \frac{\tau_1 \tau_2}{\tau_2 - \tau_1} (e^{-t/\tau_2} - e^{-t/\tau_1})$
	$\tau_1 = 1\,\text{ms}$ $\tau_2 = 8\,\text{ms}$; $E_{GABA} = -75\,\text{mV}$
	P: $\bar{g}_{GABA} = 5\,\text{nS}$; D: $\bar{g}_{GABA} = 10\,\text{nS}$